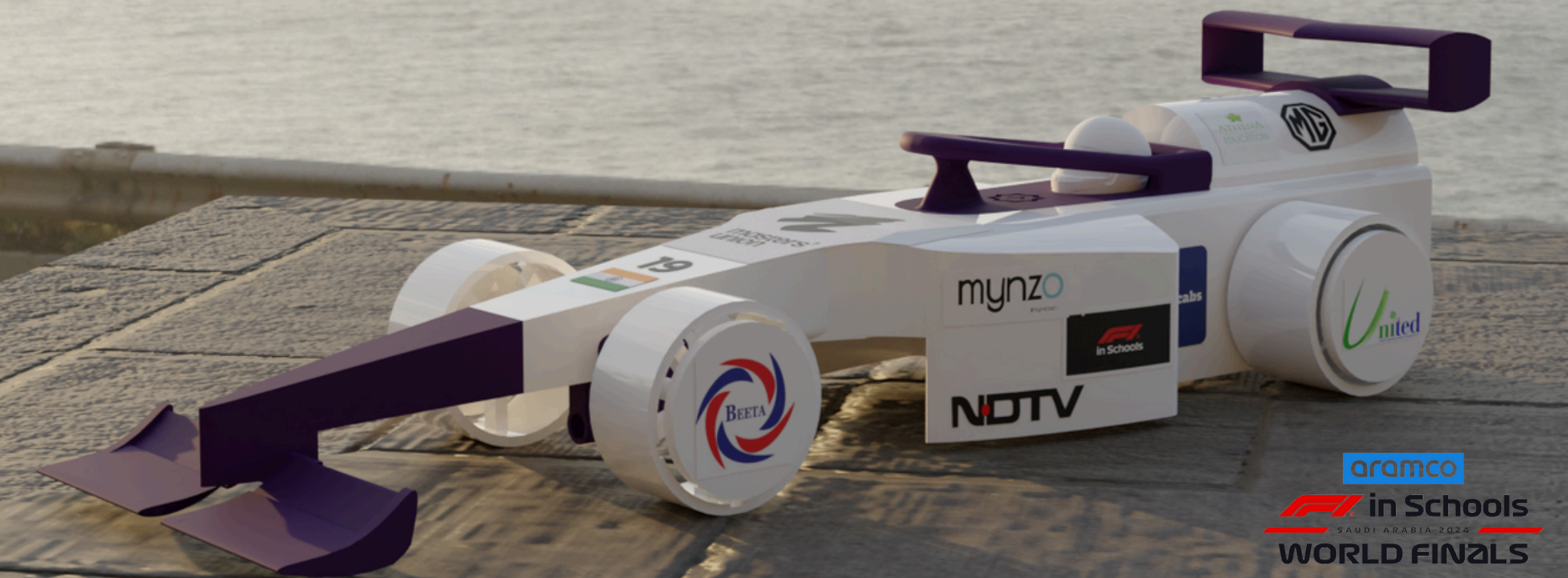


P Design and Engineering Portfolio

Photon Racing T 19

Table of contents

- Design Concepts (Page 1)
- 3D Modelling (Page 2)
- Research & Development (Page 3,4,5)
- Computer Aided Analysis (Page 6)
- Testing (Page 7)
- Use of CAM & CNC (Page 8)
- Other manufacturing & assembly (Page 9)
- Design Evaluation (Page 10)



ABEC 3 5 7

mynzo

yatra



ATHENA
EDUCATION

INDIAN
TRAVEL
HOUSE

masters'
union

NDTV



Design Concepts



Design Objectives

With our 5 years of experience in the Indian National's Competition, we laid out a set of objectives that we wanted our car to meet.

1. Maximize Car Performance: Our metric for maximum car performance was for our car to be able to achieve the best possible race times.

2. Maximize Car Reliability: Another major objective was to ensure the car stayed consistent for over 10 races. We believe this was imperative after structural issues in our National's car.

3. Ensure Car Safety and Compliance: Lastly, we wanted to ensure our car was safe to race by ensuring it complied with all the critical regulations.

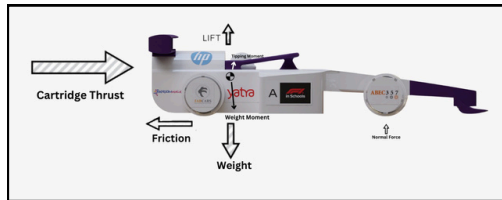


Figure 1.1: Free Body Diagram of Aura

Aerodynamics

Coanda Effect

The Coanda Effect was central to our design strategy, as it enables the airflow to "stick" to the surface contours of each car component. By implementing NACA airfoils, we were able to guide the air smoothly along the boundary layer, reducing

separation and drag. By encouraging air to follow the shape of each component, the Coanda Effect helped us streamline the aerodynamic profile, which in turn reduces the car's resistance and optimizes its efficiency on the track.

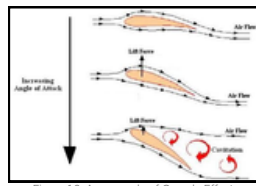


Figure 1.2: An example of Coanda Effect on Airfoils
Credit: discoverhovor.org

Cambered Airfoils (Study)

Camber refers to the curve in the airfoil profile, and adjusting this curve is key to controlling both drag and downforce. In our theoretical study, we sought to find the optimal camber percentage to achieve minimal drag and maximum downforce. Using tools provided by AirfoilTools.com,

we tested 20 similar NACA airfoils with camber percentages increasing in 0.5% increments, from 0% to 9.5%. We plotted the results for both drag and downforce and optimized them through calculus to find the ideal balance. The optimal camber was found to be 5.5%, which we applied consistently across all airfoils in the car.

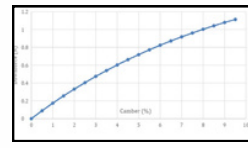


Figure 1.3: A plot of Camber vs Downforce
Credit: Photon Racing

Bernoulli's Principle

According to Bernoulli's Principle, an increase in velocity corresponds with a decrease in pressure. In aircraft design, this principle is typically applied to generate lift by creating lower pressure above the wings.

In our case, we inverted this principle to generate downforce. By designing the wings as inverted airfoils we created a higher pressure zone above the wings and lower pressure below. This pressure differential pulls the car down toward the track, increasing grip and stability at high speeds.

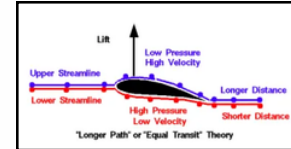


Figure 1.4: An example of Bernoulli's Principle in Airfoils
Credit: astrocamp.org

Kinematics and Dynamics

Mass

The mass of our F1 in Schools car plays a significant role in its overall performance, directly impacting acceleration, stability, and handling. A lower mass reduces inertia, enabling faster acceleration due to the decreased force required to propel the car forward.

Through careful material selection and precision machining, we aim to minimize mass without compromising strength, ensuring the car can withstand the stresses of repeated races.

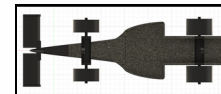


Figure 1.5: A showcase of our car's center of mass

Pitch, Yaw, and Stability

Pitch and yaw are two key aspects of a car's movement. Pitch refers to the up and down tilt of the car, which can affect forward stability, especially during acceleration. Yaw is the side-to-side rotation that causes the car to drift or veer off a straight path.

To control pitch and yaw, we maximised the wheelbase as much as possible with our design. Additionally, we tried to maximise the length of our car to ensure stability.

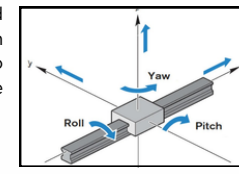


Figure 1.6: A showcase of pitch and yaw axes
Credit: discoverhovor.org

Frictional Forces

Rolling and Sliding Friction

Rolling friction occurs between the tyres and the track surface. It affects traction and grip, influencing acceleration. Optimizing rolling friction is crucial for maintaining speed and handling. Rolling friction is mainly dependent upon mass, as well as the coefficient of friction on the wheels.

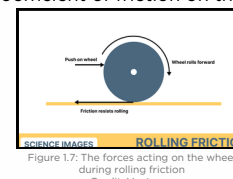


Figure 1.7: The forces acting on the wheel during rolling friction
Credit: Vecteezy

We aimed to reduce this friction as much as possible to aid our car toward the latter half of the race. When the thrust wears off, reducing friction is pivotal to faster Sector 2 times.

Structure

Structure comprises all the concepts which go into picking the correct materials which we manufacture our final car with. From our experience with various materials over the 5 years in the nationals round of this competition: ABS, PLA, PA12, etc. a major part of our research was for materials. This would help us achieve our objective of reliable car performance.

Young's Modulus

Young's modulus represents the linear relationship between stress and strain in the elastic (reversible) deformation region of a material's stress-strain curve. It describes how much a material will stretch or compress under a given load within its elastic limits.

The formula is:

$$Y = \frac{\sigma}{\epsilon} = \frac{(F/A)}{\Delta L/L}$$

Where:

- σ is stress
- ϵ is strain
- F is Force
- A is Cross-Sectional Area
- L is Length



Figure 1.8: Final Break After Elongation Test
Credit: h2o.org

Material	Density	Young's Modulus	Elongation to Break
Polyamide-12	1.01 g/cm	1.7 GPa	20%
EPS Foam	0.01-0.03 g/cm	N/A	N/A
Polypropylene	0.93 g/cm	1.3 GPa	159%

We used these concepts to come to the final choice of our material to be PA-12, after considering all other options.

3D Modelling



3D Modelling Techniques

Our techniques used evolved significantly over time, as is evinced by our disjoint generations of cars. The main body is something that evolved quite significantly, and an evaluation of the same is present below.

CAD Software Choice

Our primary CAD software choice is Autodesk Fusion 360 because of its simple and friendly UI as well as ease of changing sketches and their dimensions. It also runs on devices that cannot handle softwares of significant loads

Method	Description	Benefits	Limitations
Fit point spline + tangent + curvature handles	A series of spline points joint to create a curved line. Each point has a tangent and curvature handle used to manipulate the behaviour of the curve	Incredibly versatile, more freedom than any other tool for sketching curves	Sometimes points tend to get locked onto edges and vertices and cannot be removed without removing the entire curve
Filet & extrusion	A sequence of geometrical profiled cuts and filets.	It was easy to use, and offered separate treatment of other components and the main body	If fillets are done, no other changes can be made to the filleted components without reversing it.
Sweep	Sweeps a sketch profile, planar face, or a solid body along a selected path.	It was extremely useful in free-form extrusion of selected profiles along a path - especially for our rear wing	Certain profiles get restricted in cases of extreme sharp turns in 3D sketches. Extrapolating profiles is difficult

Airfoil Integration

Acknowledging the importance of aerofoils in our design, their prominent use is in our front and rear wings, we needed a quick and efficient way of utilizing effective airfoils throughout our design.

To facilitate this we utilized Airfoiltools.com. Their repository contains over thousands of airfoils from reputed aeronautical manufacturers like Boeing. We were able to update their profiles and import these into CAD, modifying them to best suit our purpose. The most used airfoils were the NACA 5 airfoils, prevalent in our final rear and front wings.

CAD Query

In other places of our design, we often needed to replicate designs over and over again with small tweaks to see the impact during virtual testing. Rather than going into Fusion and changing all of this manually, for repetitive modelling tasks we utilized CAD Query, allowing us to create multiple models at a very high volume.

Manufacturing Considerations

To prepare our car for manufacturing, considerations had to be taken every step of the way during 3D Modelling. As we were using the MRC40, we had access to only a 6.35 mm ball nose cutter. We used various tools to ensure that our car would be manufacturable.

Radius Analysis

We used Fusion 360's minimum radius tool to see which of our surfaces has the required radius to be machined with a 6.35 mm ball nose cutter.

Surfaces which were not abiding by this would need additional sanding during manufacturing and would have machine inconsistencies. Using this tool allowed us to mitigate this.

Draft Analysis

To ensure perfect cut depth and to see the manufacturing limits of our car, the draft analysis tool was utilized. This allowed us to see which parts of our car were accessible by the tool and enabled us to set our cut depth accordingly.

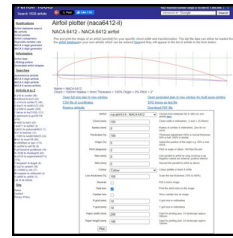


Figure 2.1: A sample airfoil created using airfoiltools.com

CAD Surface Quality

Understanding of how the surfaces of the car's body are shaped is curvature analysis. In basic terms, its scope looks at how the car's form determines its airflow. These curves are important because they help to create a better sleek design that has high stability and low drag which improves the car's aerodynamic performance.

We utilized Fusion 360's inbuilt curvature analysis to help envisage the shapes of the car and see how its sections interact with the air.

Zebra Analysis

The patterns showed if there were any abrupt changes or inconsistencies in the transitions between surfaces. Smooth, unbroken zebra stripes indicated high-quality surface continuity, while distorted or interrupted stripes highlighted areas needing refinement.

This method helped us ensure that each surface blended seamlessly with adjacent ones, optimizing the car's aerodynamic efficiency and ensuring a polished final design. Through this we located where fillets were required to smooth our car's curvature.

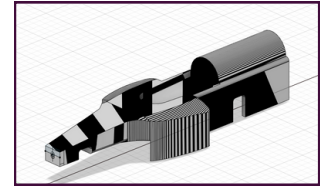


Figure 2.4: Zebra Analysis of Car Main Body

G-Continuity

Another important concept for analyzing our CAD surfaces was the use of G-Continuity. There are 3 main types of continuity, and they were used in various places throughout our design to achieve different goals:

G0 Continuity (Positional Continuity):

This is a coarse level of continuity where two surfaces join at 90 degrees. This was used in our car to ensure the gaps between the different components of the car are minimal to maximize structural integrity.

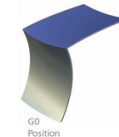


Figure 2.5: G0 Continuity
Credit: Alias Workbench

G1 Continuity (Tangential Continuity):

This level of continuity requires the 2 surfaces to meet and share a tangent at the point of contact. This ensures a smooth transition and was used in our sidepods where smooth surfaces were required to facilitate the Coanda effect.

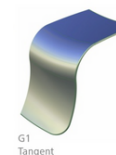


Figure 2.6: G1 Continuity
Credit: Alias Workbench

This level of continuity is the smoothest and requires a continuous rate of change of direction. This was not used as often as it was difficult to implement practically, however its utilization would have been beneficial for aerodynamic efficiency.



Figure 2.7: G2 Continuity
Credit: Alias Workbench

Research & Development



Bearings

A crucial component of any wheel system is the bearings. Many factors come into play while choosing the correct bearing for our car:

Bearing Mass

The mass of the bearings is crucial as it contributes to 2 main components: frictional force and moment of inertia. As the moment of inertia increases with mass, with heavier bearings the wheels will take longer to spin up, initially slowing the car as it skids against the track. Secondly, in ball bearings, the frictional force is due to the movement of the balls against the cage. This is due to the centrifugal force which comes about because of . A higher mass would lead to more force, increasing the friction. Hence a major goal for our bearings was to reduce the mass as much as possible.

Bearing Material

The main decision in bearing material was choosing between ceramic and hybrid ceramic bearings. While hybrid ceramics were cheaper and more sturdy, ceramic bearings provided less friction and were generally faster but more expensive. We ran a bearing test for RPM and Wheel Longevity, finding that ceramic bearings spun longer than hybrids for the same amount of torque.



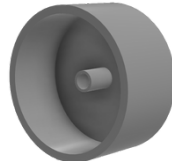
Figure 3.1: Material Analysis for bearing

Lastly, we had to choose between the ceramic material, Zirconia or Silicon Nitride. While Zirconia was the more cost-effective option, silicon nitride provided bearings with a lower dynamic friction coefficient and were more impact-resistant. Hence, we decided to go ahead with Silicon Nitride Bearings.

Wheel v1

Our initial wheel design was the simplest and was used for the India National Finals. The main reason for this choice was its finish. These wheels were supplied by the organizer and were made from ABS leading to a very smooth and professional finish. We believed this would reduce the friction against the track.

However, the wheels were very clunky and heavy, leading to a heavier car. We learnt to incorporate lighter wheels in our later car drafts.



Moment of Inertia: 350.03 g mm³
Mass: 3.5 g

Figure 3.2: Wheel V1

Wheel v2

Our next wheel design consisted of a rolling surface attached with a thin disk in the middle and a stationary cover on the other end. This approach was meant to lower the moment of inertia as less mass was now spinning. This meant that we had to machine our own wheels and had to come up with our own method to get a perfect finish.

Although the wheel had less moment of inertia than the previous iteration, the finish on these wheels were very rough as they were made from SLS Nylon. It showed us that our later drafts had to emphasize good finish to minimize friction.



Moment of Inertia: 304.62 g mm³
Mass: 2.3 g

Figure 3.3: Wheel V2

Wheel v3

Our final wheel design incorporated the idea of reducing moment of inertia and getting the perfect finish. We FDM printed these wheels out of nylon and used a rotating sander to polish these wheels evenly. The walls were the thinnest possible at 1 mm and the wheel had 5 spokes, further reducing the moment of inertia.

We chose to FDM print these wheels as there weren't many choices for materials to mill the wheels in. We felt it would be easier to sand and polish FDM printed wheels as vendors for good quality milled wheels were unavailable.



Moment of Inertia: 152.78 g mm³
Mass: 1.5 g

Figure 3.4: Wheel V3

Wheel System v1

Initially, we decided to use axle bushings in the body with the axle going through the entire body and spinning. We believed that this would be more stable however it backfired. The moment of inertia increased as the axle was also spinning and aligning the wheels was extremely difficult.



Mass: 2g
Spin Lifetime: 7.2s

Figure 3.4: Wheel System V1

Wheel System v2

Although the mass of the previous wheel system was extremely low, its lifetime and alignment were not the greatest. Hence, in our later models we decided to emphasize alignment and lifetime. This was to ensure that our car would roll straight, and not collide with the walls of the track. Additionally, as the CO2 Cartridge only brings us a third of the way, a high wheel system lifetime would ensure that the wheels get spinning fast and reliably toward the latter half of the race.

Hence our v2 wheel system featured a stationary axle and a separate housing that slots into the main body. The axle is attached to rotating wheels with bearings. With this the rotating mass is minimized, further lowering moment of inertia.



Mass: 5.2g

Spin Lifetime: 24.5s

Figure 3.5: Wheel System V2

Wheel System v3

For our final wheel system, we sought to minimize the impact of wake. One way to implement this was to add a wheel cover at the end of the wheel system. This covered up the exposed, spinning interior of the wheels, allowing the air to flow away from it, reducing the wheel wake that was realized.

Additionally, as we were dealing with issues in mass management as well as keeping an equal axle length on either side, we decided to keep our wheel system with 2 separate axles. This helped reduce all of our issues with alignment and mass. One thing we could've implemented, however, is to create a solid wall. This would reduce manufacturing issues and simplify the glueing process. Additionally, we added the tetherline guide at the bottom, combining components and reducing mass.



Mass: 4.3g

Spin Lifetime: 26.3s

Figure 3.6: Wheel System V3

Summary

Our final wheel system utilized the following guiding principles and design concepts:

1. Minimize Moment of Inertia
2. Minimize Rolling Friction (Use of Ceramic Bearings)
3. Reduce Mass

Based on these principles, we used Wheel v3 and Wheel System v3 and are confident that they enabled us to perform well in Sector 2 of the race.

Research & Development



Thrust Profiling

A pivotal step in our car design process was modelling the entire race using thrust profiling.

Step 1:

With the help of ideal gas equations adjusted for real gas effects using the Peng-Robinson equation, we were able to calculate the initial conditions and actual molar mass and pressure of the CO₂.

Step 2: Assuming for real gas effects using Peng-Robinson

$$P = \frac{RT}{V - b - \frac{a}{(T + b)}} \quad (1)$$

$$a = 0.420 \frac{RT^2}{V^2 + 2bV + b^2} \quad (2)$$

$$b = 0.0778 \frac{RT}{V + b} \quad (3)$$

$$m_{CO_2} = \frac{P}{RT} M_{CO_2} \quad (4)$$

Step 2:

With the help of ideal gas equations adjusted for real gas effects using peng-robinson equation, we were able to calculate the initial conditions and actual molar mass and pressure of the CO₂.

Step 3:

Then Partial Differential Equations for continuity, momentum conservation, rate of change of energy per unit volume, divergence of energy flux, heat dissipation and energy conservation were used to write pressure as a function of volume of CO₂ gas released

Parameters were added to these equations and then they were discretized using finite difference method. The nozzle length was divided into discrete segments and time-stepping (euler's method) was conducted with small intervals of t. We therefore get time-dependent profiles of pressure, density and velocity. These profiles are inputs for calculating the mass flow rate and thrust at each time step - helping to generate a thrust profile over time

Using the data calculated from step 4, it was input into step 2, where pressure and density of the gas were adjusted for real gas properties. Step 2 was solved from step 4 values at each time step, getting a time profile.

Adjusted density and velocity as functions of the gas are then input into the formula for mass flow rate. Then using newton's second law of Force = mass * acceleration, the instantaneous thrust is calculated. Where mass is mass flow rate and momentum is used instead of acceleration to calculate thrust

Step 3: Initial conditions & mass calculation of CO₂

- Create Variables
- Calculate Molar (m) using ideal gas equation
- $m = \frac{P \cdot V}{R \cdot T} \cdot M_{CO_2}$
- Calculate Mass
- $m_{CO_2} = \frac{P}{R \cdot T} \cdot M_{CO_2}$

Car Prototypes

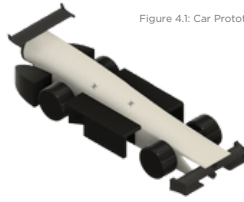


Figure 4.1: Car Prototype V1



Figure 4.3 Car Prototype V3

Prototype B

Mass: 46.1g

Best Drag Force Achieved: 0.41N
Best Race Time: N/A

Solara

Mass: 50.2g

Best Drag Force Achieved: 0.51N
Best Race Time: 1.21s

Our Thought Process:

Solara's main goal was to achieve a smooth, aerodynamic design with minimal drag for optimal speed and stability. Its defining feature was an innovative lofted design, transitioning smoothly from cylindrical to cuboidal, which enhanced aerodynamic efficiency.

Design Concepts Utilized:

Our approach focused on both qualitative and quantitative aspects, incorporating features like wheel wake, flow separation, and vortices. The front wing, shaped with Bezier curves and differential equations, guided airflow around and through the car efficiently. Built as a separate CAD component, it allowed for easy adjustments.

Our Learnings:

However, the loft design added excessive weight and complexity, particularly in the front wing and main body. This experience taught us the importance of balancing innovation with practicality, leading us to focus on lighter, more efficient designs in future iterations.



Figure 4.4 Car Prototype V4

Prototype C: Aura

Mass: 43.1g

Best Drag Force Achieved: 0.30N
Best Race Time (older version): 0.83s

Zeta

Mass: 47.8g

Best Drag Force Achieved: 0.47N
Best Race Time: N/A

Our Thought Process:

Zeta's goal was to refine Solara's design by addressing its aerodynamic inefficiencies. The defining feature was an optimized, lighter form that retained key aerodynamic properties for high-speed performance, making Zeta a more efficient replacement for Solara.

Design Concepts Used:

Using mentor feedback, we refined the loft into a simpler, tapered shape to improve airflow without added bulk. The front wing, redesigned in Fusion 360, maintained aerodynamic effects with a streamlined structure, while sidepods inspired by fifth-generation jets directed airflow inward for better stability. We also introduced a new, high-performing rear wing inspired by World Finals teams.

Our Learnings:

Although simpler, Zeta's cuboidal front profile limited its aerodynamic potential, highlighting the need for further refinements.

Step 4: Calculating the front profile for a smooth transition from the front to the main body

- Create a new profile
- Solve for m_{CO_2} from data of step 4 for each time step, getting a front profile
- Use the adjusted density & velocity at each time step to calculate the front profile
- $m_{CO_2} = \frac{P}{R \cdot T} \cdot M_{CO_2}$
- $\rho = \frac{m}{V}$
- $\rho = \frac{P}{R \cdot T}$
- $\rho = \frac{P}{R \cdot T} \cdot M_{CO_2}$
- $\rho = \frac{P}{R \cdot T} \cdot M_{CO_2}$

Step 5: Calculating the front profile for a smooth transition from the front to the main body

- Create a new profile
- Solve for m_{CO_2} from data of step 4 for each time step, getting a front profile
- Use the adjusted density & velocity at each time step to calculate the front profile
- $m_{CO_2} = \frac{P}{R \cdot T} \cdot M_{CO_2}$
- $\rho = \frac{m}{V}$
- $\rho = \frac{m}{V}$
- $\rho = \frac{m}{V}$
- $\rho = \frac{m}{V}$

Figure 4.2: Car Prototype V2

Step 6: Calculating the front profile for a smooth transition from the front to the main body

- Create a new profile
- Solve for m_{CO_2} from data of step 4 for each time step, getting a front profile
- Use the adjusted density & velocity at each time step to calculate the front profile
- $m_{CO_2} = \frac{P}{R \cdot T} \cdot M_{CO_2}$
- $\rho = \frac{m}{V}$
- $\rho = \frac{m}{V}$
- $\rho = \frac{m}{V}$
- $\rho = \frac{m}{V}$

Figure 4.3: Car Prototype V3

Step 1: Initial Conditions & Mass Calculation of CO_2 .

→ Given Parameters

→ Calculate Moles (n) using Ideal Gas Equation

$$n = \frac{P_{\text{initial}} \times V_{\text{cartridge}}}{R \times T_{\text{initial}}}$$

→ Calculate Mass

$$m_{\text{CO}_2} = n \times M_{\text{molar mass CO}_2}$$

Step 2: Adjusting for Real Gas Effects using Peng-Robinson EOs

$$P = \frac{RT}{V_m - b} - \frac{a}{(V_m^2 + 2bV_m - b^2)}$$

Here, $a = 0.45724 \frac{R^2 T_c^2}{P_c}$ } (T_c & P_c = critical values for CO_2)

$$b = 0.0778 \cdot \frac{RT_c}{P_c}$$

V_m = Molar volume used to account for real gas behaviour.

$$P_{\text{initial}} = \frac{1}{V_m} \rightarrow \text{molar mass of CO}_2$$

$$\frac{\partial(\rho E)}{\partial t} = \text{Rate of change of Energy per unit volume with time}$$

$$\nabla \cdot ((\rho E + P) \mathbf{v}) = \text{Divergence of the energy flux (including internal energy & work done by pressure.)}$$

$$\nabla \cdot (k \nabla T) = \text{Heat conduction term.}$$

↑
Thermal conductivity of CO_2 Temp gradient

$$\phi = \text{Viscous dissipation function.}$$

(Energy lost due to viscous effect.)

→ Discretize the Equations:

- Use a numerical method (like FVM or FDM)
- Divide the nozzle length into discrete segments and apply time-stepping (Euler's Method) with small interval Δt
- Apply Boundary condition like Inlet & Outlet conditions.

Note: By the end of Step ③, we get time-dependent profiles of pressure, density & velocity. These profiles are inputs for calculating the mass flow rate & thrust at each time step.

↑
Instead of a single thrust value, it helps generate thrust profile over time.

Step 4: Calculating Real Gas-Adjusted Density & Pressure --
at Each time step.

~~relative for pressure~~

→ solve step 2) from data of step 4) for
each time step, getting a time profile.

Step 5: Instantaneous Mass flow Rate.

(use the adjusted density & velocity at
the nozzle exit at each time step from
step 3))

$$\dot{m} = \dot{m}_{exit} \cdot A_{exit} \cdot v_{exit}$$

\dot{m}_{exit} ←
mass flow rate
calculate from
step 3) from each time step

Step 6: Instantaneous Thrust

$$F_{inst} = \dot{m} v_{exit} + (P_{exit} - P_{ambient}) \cdot A_{exit}$$

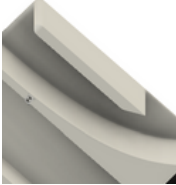
Note: to get time-dependent thrust profile, this would at time
do steps 1) to step 5). This would look like $\begin{cases} 0s \rightarrow \text{some } N \\ 1.5s \rightarrow \text{some } N \\ 3s \rightarrow \text{some } N \end{cases}$

Research & Development



Sidepods

V1 (Channelled Outwards)

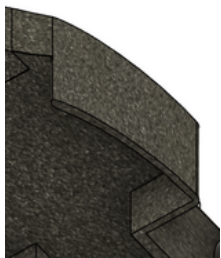


Our Thought Process:
The first version of the sidepods was designed to channel air outward, directing airflow away from the wheels to reduce wheel wake.

Design Concepts Used:
We wanted to redirect the air from our wheels and minimize the amount of wheel wake.

Our Learnings:
However, mentor feedback indicated that the redirected air could hit the track walls, potentially causing lateral forces that might destabilize the car. During testing, it became evident that most incoming airflow bypassed the channels, flowing along the car's outer surface instead, which reduced the effectiveness of this design. The limited airflow through the channels led to underwhelming results, and the observed lateral force slightly disrupted the car's straight-line stability. Outward-facing channels were crafted to prevent air from hitting the wheels, aiming to improve stability.

V2 (Hollowed Sidepods)



Our Thought Process:
This sidepod design took a different approach, prioritizing weight reduction over complex channeling. These sidepods were hollowed out, which reduced overall weight and provided basic coverage for the rear wheels.

Design Concepts Used:
The smoother, swept surfaces of this design minimized drag and helped prevent vortex formation. By removing excess material, this design achieved significant weight savings, which positively impacted speed and performance.

Our Learnings:
The simplified, lightweight design ultimately proved that a focus on reducing weight could yield more effective results than intricate channeling.

Front Wing

Wing v1 (3-Way Manipulation)



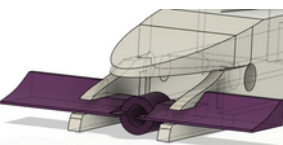
Design Concepts Used:

This design allowed for maximum utilization of the Coanda effect in both the up-down and left-right directions, with a simple structure in place to ensure clean flow separation and adherence to regulations.

Our Learnings:

However, this wing was quite complex, and the excessive manipulation of airflow actually increased surface drag. Additionally, the splines were not optimized for the Coanda effect, limiting the effectiveness of the design.

Wing v2 (Single Elevated Wing)



This wing was designed to eliminate redundancies identified in the 3-way wing. It consisted of a single, manually cambered airfoil shaped with a spline, although this spline was not ideal for maximizing the Coanda effect. Despite this, the wing's joint was easy to install and structurally stable. However, its weight was notably high due to the bulky rear side, which added unnecessary mass.

Wing v3 (Double vaned Cambered NACA Wing)

Our Thought Process:
We wanted to achieve a good flow separation and increase the redirection of air through the use of this prototype.

Design Concepts Used:

For this version, we used NACA airfoils with a camber of 5.5% and an angle of attack (AoA) of 10 degrees for the lower vane, and a camber of 9.5% with an AoA of 10 degrees for the upper vane, to direct air as far away from the wheels as possible. The camber and AoA were optimized through a focused study, allowing for maximum Coanda effect with smoother airflow.

Our Learnings:

This design also had a lower mass and a simpler structure, making it more efficient and easier to manage than the previous version.

Rear Wing



Symmetric Elliptical Airfoil

Our Thought Process:

The elliptical airfoil, with its fully symmetrical shape, is straightforward to manufacture. Its lack of complex curves means it's simple to install, which can be a big advantage, especially because better manufacturing quality is essential for preventing breakages on the track.

Design Concepts Used:

Because of its low frontal area, it also creates a lesser air resistance when positioned with the flow, which helps with basic aerodynamics. But this design has real drawbacks when mounted on a car. Since it's symmetrical and lacks camber, it can't create downforce, which is crucial for stability and grip, especially at higher speeds.

Our Learnings:

Furthermore, the round leading edge can disrupt airflow, causing separation and turbulence. This turbulence increases drag, which is why other airfoils were suited better for the rear wing.



Double Vaned Wing

Our Thought Process:
This rear wing was designed to apply Bernoulli's principle by reducing the frontal area as air moved through it, using two manually cambered airfoils.

Design Concept Used:

The upper airfoil was set at a positive 10-degree angle and the lower one at a negative 10-degree angle. This design aimed to create a pressure differential for downforce.

Our Learnings:

While it performed better than the previous symmetrical elliptical airfoil, simulations showed that Bernoulli's principle wasn't fully realized, as there was no significant change in velocity. Additionally, the sharp edges at the wing's end created unwanted vortices, impacting overall aerodynamics.



Raptor Wing

Our Thought Process:
Our final rear wing design used three different NACA airfoils seamlessly connected to resemble a double-vaned, streamlined wing.

Design Concepts Used:

The upper and lower airfoils were cambered at 5.5%, identified as the optimal camber to maximize downforce and minimize drag based on airfoiltools.com data. A notable addition was the use of airfoil-shaped endplates with a low camber of 1.5%, aiding in smooth airflow guidance and applying the Coanda effect. The wing's shape, inspired by the thrusters of an F22 Raptor, was created using the sweep function, featuring a sharp centre and curved edges to cut through and direct airflow efficiently.

This design offered enhanced aerodynamic performance by balancing downforce with minimized drag.

Computer Aided Analysis



Testing Process

Throughout the design process, we meticulously documented each testing phase in a spreadsheet, allowing us to track the results systematically and identify trends in our data. By organizing our tests in this manner, we could monitor each parameter's effect on the overall performance, making it easier to fine-tune individual components.

Each component of the car was tested independently and integrated into each body iteration. To determine the most efficient configurations, we tested various assembled cars to optimize drag and stability, particularly focusing on aerodynamics and weight distribution. This approach, though ambitious, allowed us to reach the final configuration by balancing various parameters, helping to enhance both speed and control.

Virtual Wind Tunnel Testing

Virtual wind tunnel testing was a critical step in assessing the car's aerodynamic performance. By simulating wind flow over a stationary car model (as opposed to moving the car itself), we could mimic real-world conditions and evaluate drag and lift forces on the car body. This method enabled us to observe airflow behavior at a speed like what the car would experience on the track. For a comprehensive analysis, we conducted these tests across three different software platforms—Ansys Discovery, SolidWorks Flow Simulation, and Autodesk CFD Ultimate—to leverage their unique features and validate our results.

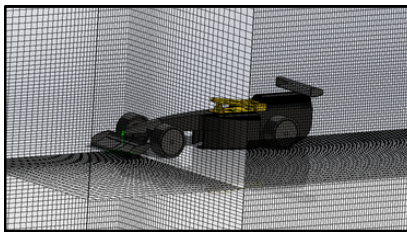


Figure 6.2: Car Virtual Wind Tunnel Environment + Mesh

Mesh Convergence Study

One of the most essential parameters in our CFD process was our mesh. To ensure accuracy we conducted a mesh convergence study. In CFD simulations, mesh convergence is crucial because the mesh affects the precision of the simulation. A finer mesh captures more detail in complex areas but requires more computational resources, whereas a coarser mesh reduces computational load but may miss important flow details.

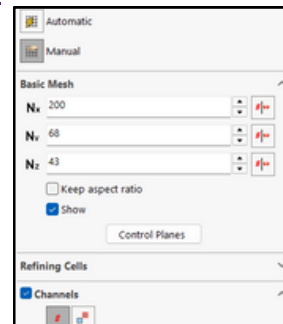
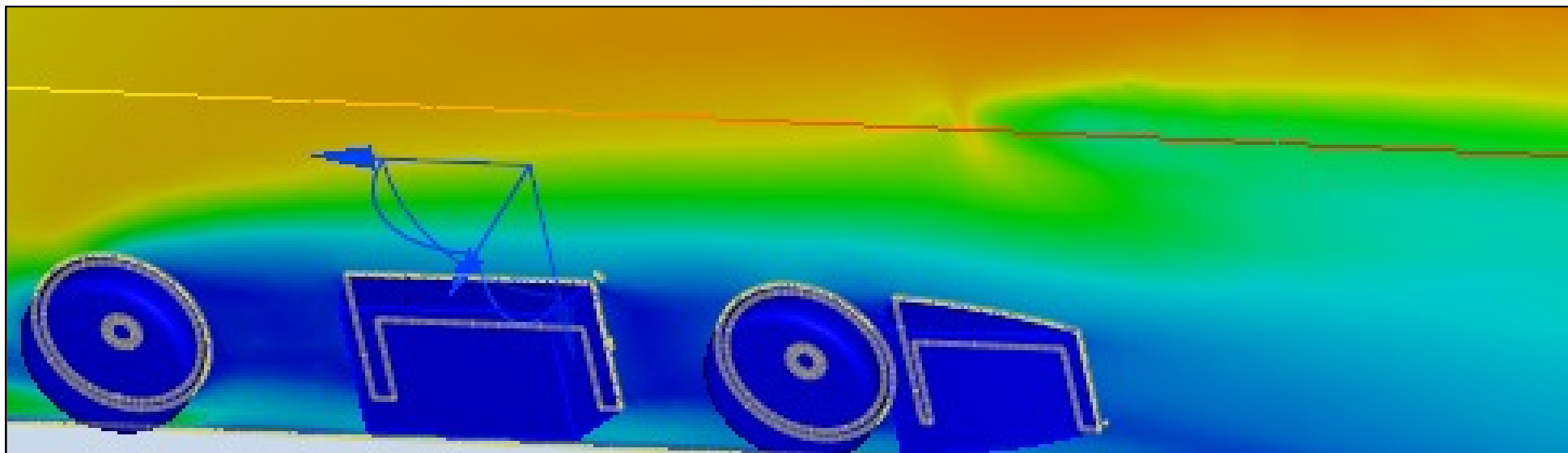


Figure 6.3: Mesh convergence settings

Procedure Name	Drag Force	Turbulence	Mesh Setting
Front	0.0001	10%	1
Front	0.0002	10%	2
Front	0.0003	10%	3
Front	0.0004	10%	4
Front	0.0005	10%	5
Front	0.0006	10%	6
Front	0.0007	10%	7
Front	0.0008	10%	8
Front	0.0009	10%	9
Front	0.0010	10%	10
Front	0.0011	10%	11
Front	0.0012	10%	12
Front	0.0013	10%	13
Front	0.0014	10%	14
Front	0.0015	10%	15
Front	0.0016	10%	16
Front	0.0017	10%	17
Front	0.0018	10%	18
Front	0.0019	10%	19
Front	0.0020	10%	20
Front	0.0021	10%	21
Front	0.0022	10%	22
Front	0.0023	10%	23
Front	0.0024	10%	24
Front	0.0025	10%	25
Front	0.0026	10%	26
Front	0.0027	10%	27
Front	0.0028	10%	28
Front	0.0029	10%	29
Front	0.0030	10%	30
Front	0.0031	10%	31
Front	0.0032	10%	32
Front	0.0033	10%	33
Front	0.0034	10%	34
Front	0.0035	10%	35
Front	0.0036	10%	36
Front	0.0037	10%	37
Front	0.0038	10%	38
Front	0.0039	10%	39
Front	0.0040	10%	40
Front	0.0041	10%	41
Front	0.0042	10%	42
Front	0.0043	10%	43
Front	0.0044	10%	44
Front	0.0045	10%	45
Front	0.0046	10%	46
Front	0.0047	10%	47
Front	0.0048	10%	48
Front	0.0049	10%	49
Front	0.0050	10%	50
Front	0.0051	10%	51
Front	0.0052	10%	52
Front	0.0053	10%	53
Front	0.0054	10%	54
Front	0.0055	10%	55
Front	0.0056	10%	56
Front	0.0057	10%	57
Front	0.0058	10%	58
Front	0.0059	10%	59
Front	0.0060	10%	60
Front	0.0061	10%	61
Front	0.0062	10%	62
Front	0.0063	10%	63
Front	0.0064	10%	64
Front	0.0065	10%	65
Front	0.0066	10%	66
Front	0.0067	10%	67
Front	0.0068	10%	68
Front	0.0069	10%	69
Front	0.0070	10%	70
Front	0.0071	10%	71
Front	0.0072	10%	72
Front	0.0073	10%	73
Front	0.0074	10%	74
Front	0.0075	10%	75
Front	0.0076	10%	76
Front	0.0077	10%	77
Front	0.0078	10%	78
Front	0.0079	10%	79
Front	0.0080	10%	80
Front	0.0081	10%	81
Front	0.0082	10%	82
Front	0.0083	10%	83
Front	0.0084	10%	84
Front	0.0085	10%	85
Front	0.0086	10%	86
Front	0.0087	10%	87
Front	0.0088	10%	88
Front	0.0089	10%	89
Front	0.0090	10%	90
Front	0.0091	10%	91
Front	0.0092	10%	92
Front	0.0093	10%	93
Front	0.0094	10%	94
Front	0.0095	10%	95
Front	0.0096	10%	96
Front	0.0097	10%	97
Front	0.0098	10%	98
Front	0.0099	10%	99
Front	0.0100	10%	100
Front	0.0001	10%	101
Front	0.0002	10%	102
Front	0.0003	10%	103
Front	0.0004	10%	104
Front	0.0005	10%	105
Front	0.0006	10%	106
Front	0.0007	10%	107
Front	0.0008	10%	108
Front	0.0009	10%	109
Front	0.0010	10%	110
Front	0.0011	10%	111
Front	0.0012	10%	112
Front	0.0013	10%	113
Front	0.0014	10%	114
Front	0.0015	10%	115
Front	0.0016	10%	116
Front	0.0017	10%	117
Front	0.0018	10%	118
Front	0.0019	10%	119
Front	0.0020	10%	120
Front	0.0021	10%	121
Front	0.0022	10%	122
Front	0.0023	10%	123
Front	0.0024	10%	124
Front	0.0025	10%	125
Front	0.0026	10%	126
Front	0.0027	10%	127
Front	0.0028	10%	128
Front	0.0029	10%	129
Front	0.0030	10%	130
Front	0.0031	10%	131
Front	0.0032	10%	132
Front	0.0033	10%	133
Front	0.0034	10%	134
Front	0.0035	10%	135
Front	0.0036	10%	136
Front	0.0037	10%	137
Front	0.0038	10%	138
Front	0.0039	10%	139
Front	0.0040	10%	140
Front	0.0041	10%	141
Front	0.0042	10%	142
Front	0.0043	10%	143
Front	0.0044	10%	144
Front	0.0045	10%	145
Front	0.0046	10%	146
Front	0.0047	10%	147
Front	0.0048	10%	148
Front	0.0049	10%	149
Front	0.0050	10%	150
Front	0.0051	10%	151
Front	0.0052	10%	152
Front	0.0053	10%	153
Front	0.0054	10%	154
Front	0.0055	10%	155
Front	0.0056	10%	156
Front	0.0057	10%	157
Front	0.0058	10%	158
Front	0.0059	10%	159
Front	0.0060	10%	160
Front	0.0061	10%	161
Front	0.0062	10%	162
Front	0.0063	10%	163
Front	0.0064	10%	164
Front	0.0065	10%	165
Front	0.0066	10%	166
Front	0.0067	10%	167
Front	0.0068	10%	168
Front	0.0069	10%	169
Front	0.0070	10%	170
Front	0.0071	10%	171
Front	0.0072	10%	172
Front	0.0073	10%	173
Front	0.0074	10%	174
Front	0.0075	10%	175
Front	0.0076	10%	176
Front	0.0077	10%	177
Front	0.0078	10%	178
Front	0.0079	10%	179
Front	0.0080	10%	180
Front	0.0081	10%	181
Front	0.0082	10%	182
Front	0.0083	10%	183
Front	0.0084	10%	184
Front	0.0085	10%	185
Front	0.0086	10%	186
Front	0.0087	10%	187
Front	0.0088	10%	188
Front	0.0089	10%	189
Front	0.0090	10%	190
Front	0.0091	10%	191
Front	0.0092	10%	192
Front	0.0093	10%	193
Front	0.0094	10%	194
Front	0.0095	10%	195
Front	0.0096	10%	196
Front	0.0097	10%	197
Front	0.0098	10%	198
Front	0.0099	10%	199
Front	0.0100	10%	200
Front	0.0001	10%	201
Front	0.0002	10%	202
Front	0.0003	10%	203
Front	0.0004	10%	204
Front	0.0005	10%	205
Front	0.0006	10%	206
Front	0.0007	10%	207
Front	0.0008	10%	208
Front	0.0009	10%	209
Front	0.0010	10%	210
Front	0.0011	10%	211
Front	0.0012	10%	212
Front	0.0013	10%	213
Front	0.0014	10%	214
Front	0.0015	10%	215
Front	0.0016	10%	216
Front	0.0017	10%	217
Front	0.0018	10%	218
Front	0.0019	10%	219
Front	0.0020	10%	220
Front	0.0021	10%	221
Front	0.0022	10%	222
Front	0.0023	10%	223
Front	0.0024	10%	224
Front	0.0025	10%	225
Front	0.0026	10%	226
Front	0.0027	10%	227
Front	0.0028	10%	228
Front	0.0029	10%	229
Front	0.0030	10%	230
Front	0.0031	10%	231
Front	0.0032	10%	232
Front	0.0033	10%	233
Front	0.0034	10%	234
Front	0.0035	10%	235
Front	0.0036	10%	236
Front	0.0037	10%	237
Front	0.0038	10%	238
Front	0.0039	10%	239
Front	0.0040	10%	240
Front	0.0041	10%	241
Front	0.0042	10%	242
Front	0.0043	10%	243
Front	0.0044	10%	244
Front	0.0045	10%	245
Front	0.0046	10%	246
Front	0.0047	10%	247
Front	0.0048	10%	248
Front	0.0049	10%	249
Front	0.0050	10%	250
Front	0.0051	10%	251
Front	0.0052	10%	252
Front	0.0053	10%	253
Front	0.0054	10%	254
Front	0.0055	10%	255
Front	0.0056	10%	256
Front	0.0057	10%	257
Front	0.0058	10%	258
Front	0.0059	10%	259
Front	0.0060	10%	260
Front	0.0061	10%	261
Front	0.0062	10%	262
Front	0.0063	10%	263
Front	0.0064	10%	264
Front	0.0065	10%	265
Front	0.0066	10%	266
Front	0.0067	10%	267
Front	0.0068	10%	268
Front	0.0069	10%	269
Front	0.0070	10%	270
Front	0.0071	10%	271
Front	0.0072	10%	272
Front	0.0073	10%	273
Front	0.0074	10%	274
Front	0.0075	10%	275
Front	0.0076	10%	276
Front	0.0077	10%	277
Front	0.0078	10%	278
Front	0.0079	10%	279
Front	0.0080	10%	280
Front	0.0081	10%	281
Front	0.0082	10%	282
Front	0.0083	10%	283
Front	0.0084	10%	284
Front	0.0085	10%	285
Front	0.0086	10%	286
Front	0.0087	10%	287
Front	0.0088	10%	288
Front	0.0089	10%	289
Front	0.0090	10%	290
Front	0.0091	10%	291
Front	0.0092	10%	292
Front	0.0093	10%	293
Front	0.0094	10%	294
Front	0.0095	10%	295
Front	0.0096	10%	296
Front			

Turbulence Parameters

Parameters	Turbulence intensity and length
Turbulence intensity	5 %
Turbulence length	0.000302759174 m



Testing



Track Testing

One of the most effective ways to test car performance was through track testing. It painted the most accurate picture of our car's performance as it would be completely realistic, accounting for the smallest discrepancies in virtual testing.

We used our organizer's F1 In School track and official Denford Race Power Packages to ensure accuracy to official races. We stuck to the official F1 In School's race protocol to ensure accuracy in the final races.

Purpose & Findings:

Our track testing was pivotal in understanding the intricacies of our car. It showed us critical issues like breakages. An example was the breakage of our axle, compelling us to increase the depth of the axle slot in the wheel support system.

We entered track testing with a set of variables which we felt could swing either way. Below is a table documenting all our expected and unexpected takeaways from track testing.

Variables	Expected Outcome	Actual Outcome
Nose cone joint structural integrity	We thought that the nose cone joint could've easily broken on impact with the deceleration system.	The nose cone joint was one of the strongest joints, being able to sustain 8 rounds of track testing without failures.
Regulation compliance	We believed that our car was compliant with almost all the regulations before track testing	At track testing we found that our car was breaking tether line safety regulations, prompting us to refine our design further.
Final prototype track testing race time	We believed that our car would achieve a track testing time of 1.00 seconds.	Our final track testing car achieved times of 0.83 seconds during track testing.

Additionally, track testing provided us with important insights for our car's thrust profiling. We were able to use video analysis on our car's races and track the smoke let out by the CO2 Canister. Tracking this smoke gave us an accurate time value for how long the CO2 Canister provides thrust. We used this information further in our thrust profiling to aid R&D and design choices.



Figure 7.2: Video Analysis of CO2 Thrust
Credit: Photon Racing

Wind Tunnel Testing

We utilized wind tunnel testing for a qualitative analysis of our car's interface with the air around it. This analysis was only qualitative as we required access to a load sensor for a quantitative analysis, which was proving to be extremely difficult due to logistical issues. However, the qualitative data still told us many things.



Figure 7.3: Wind Tunnel Testing

Variables	Expected Outcome	Actual Outcome
Clear flow visualization	We expected the flow to be quite faint and not provide much valuable insight.	The atomized water when under light was extremely visible and showed a visible interface between air and our car body.
Conceptual Understanding	Before wind tunnel testing, we believed that the results from the traces function would be extremely like wind tunnel visualization	We found many discrepancies compared to virtual tests, like at the back of our car where the exit was more turbulent than expected, allowing us to tweak our car's shape.

Stress Testing

We tested the strength and practicality of our joints by performing stress tests as outlined in the competition regulations. Each joint was loaded with the specified weight, and potential weak points were evaluated using a 500-gram weight. Key components tested included the halo, nose cone joint, and wheel support systems to assess breakage risks and ensure compliance with scrutineering requirements.



Figure 7.4: Nose Cone Stress Testing Rig

Variables	Expected Outcome	Actual Outcome
Rear wing attachment	We felt that the way our rear wing was attached was very efficient and would have minimum breakage chances.	However, under a 500-gram weight, the rear wing was deforming. Hence, we increased the surface area for gluing to increase strength.
Wheel support system	We believed that the wheel support system would be somewhat weak. Since there was only a small gluing area, we felt that it could fall out.	The wheel support system was also supported by the friction with the main body. We then figure out ways to easily detach it using a box cutter for replacing breakages.

Materials Testing

One of our methods to achieve our design objective for performance was by using the most suitable materials. One way to achieve this was by choosing the lightest materials for our external components.

We wanted to replicate an EPS Core Sandwich, a panel known for its light weight yet structural integrity.

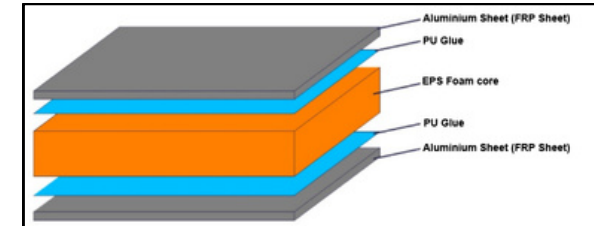


Figure 7.5: Inspiration for EPS Core Sandwich

Credit: L2 Panels

We replicated this by using medical gauze coated around a piece of foam and sealed in place with a lightweight epoxy. Although there were many logistical issues with epoxy curing time, the final surface was strong, lightweight, and durable.



Figure 7.6: Universal Testing Machine
Credit: Wikipedia

We contacted universities to utilize their Universal Testing Machine however were unable to secure a time to test the material. Instead, we did a comparative analysis with materials we already had on hand such as PETG.



Figure 7.7: EPS Compressive Ductility Test

We conducted various tests with these materials using household items. As our school labs were busy for our IBDP Assessments, we fashioned many testing apparatus on our own to get a greater understanding of the limitations of the materials and the plausibility of its usage.

We found that the cured EPS was extremely lightweight by a factor of 10 compared to thermoplastics. Additionally, the EPS had impressive compressional ductility, being able to take impacts exceptionally well compared to PLA and PETG.

Although the material was up to spec, it was extremely difficult to laminate it with epoxy as our components' geometries were complex, leading to uneven epoxy coating and errors while milling the EPS Foam. Hence, we decided to abandon this material avenue.



Figure 7.8: Epoxy treatment process

Use of CAM & CNC



Machining Goals

Moving into the manufacturing process, we decided to progress from our original design objectives into our machining goals:

Maximize Car Performance --> Ensure the car is 50 grams

Maximize Car Reliability --> Ensure apt wall thickness and strong joints

Ensure Compliance and Safety --> Keep tolerances as low as possible

CNC Router

We utilized the F1 In Schools' India organizer's MRC 40, 3-axis CNC router. It had an adequate bed size of 875x750x675 mm, with ample room to machine fine details. With its high spindle speed of 29,000 RPM, the router was able to shape the small, intricate details on the F1 car model.



Figure 8.1: A sample image of the MRC 40 CNC Router.

Credit: TechLabs.com

This high-speed capability ensures smoother finishes, essential for maximizing performance. The fast 3D profiling speed of 4,500 mm/min allowed for efficient machining of contoured surfaces, especially useful for crafting aerodynamic shapes on the car like our loft

Use of CAM Software

For our manufacturing process, we utilized the software QuickCAM Pro.

1. QuickCAM Pro was used to create the G-Code for the router. A few parameters were set specifically to achieve our machine goals and to best utilize our router.

2. Additionally, we used it to simulate the tool paths for all our machining plans, allowing the team to get a better insight into how our car would be manufactured.

3. As QuickCAM Pro was a Denford Software, we were able to use the inbuilt functions to machine our cars easier.

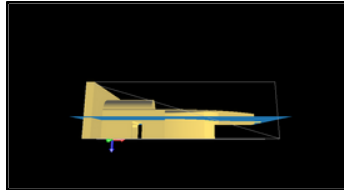


Figure 8.2: The cut depth for one of our main bodies on QuickCAM Pro

Parameters

In QuickCAM Pro, although we planned to use a much lower stepover rate, around 5 or 7%, we had to choose 14%. This was due to the limitations of the MRC40 and led to machine lines. These lines and imperfections were sanded down for a smoother finish. Additionally, we used a high spindle speed of 25,000RPM during the finishing plans to ensure accuracy and precise cuts, keeping our car faithful to the engineering drawings.

Machining Plan

For our F1 in Schools car, the machining plan using the MRC40 CNC router is designed to maximize accuracy and structural integrity, in line with our goals of maintaining low tolerances and ensuring strong joints for stability.

1. Top Machining: First, we use raster roughing on the top surface of our car at a high feed rate to create its shape. Next, we go back for another pass of raster finishing, at a high spindle speed to create a smooth finish.

2. Bottom Machining: To hollow out the cavities on the underside of our car we use bottom machining. We begin with a raster roughing before finishing off with a raster finish for a clean and smooth finish.

3. Side Machining: We used the Car Wizard function in QuickCAM Pro to do our LHS and RHS Machining. This would make the holes for our wheels system and machine the contour on our side pods.

Using all 3 axes offered by the MRC 40 allowed us to achieve the best possible finish with the hardware at hand.



Figure 8.3: Manufacturing Inconsistencies



Figure 8.4: Sample of machine lines

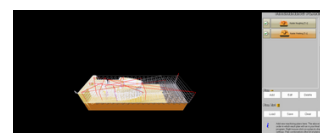


Figure 8.5: Machine Plan

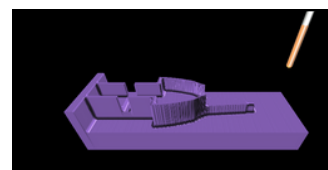


Figure 8.6: Toolpath Simulation

Issues during Machining

Our manufacturing process did not run smoothly at all. We ran into many separate issues during manufacturing which had to be mitigated to create a final car body which met all of our machining and design goals.

Initially we had issues with a visible line down through our car. This was due to improper cut depths. This issue was mitigated by using accessibility analysis on Fusion 360 as well as setting slightly higher cut depths. This ensured that our other car bodies didn't face this issue and had a smooth surface which required minimum sanding.



Figure 8.7: Bad Cut Depth

Furthermore, we also faced numerous issues with our car design. As a part of our car design, we tried our best to keep all model block constraints in mind. However, for our final car, we had to change the CO2 Cartridge Position to 27 mm and the depth to 48 mm. This was proving to be quite a challenge for the machine as there was a pre-manufactured CO2 Canister hole in the model block. This led to many issues such as the drill bit hitting the bed and sometimes switching axes too early and snapping the car.



Figure 8.10: Model Block Addition for Machining

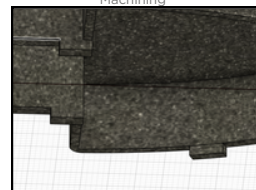


Figure 8.11: 2mm Machining Standoffs

This issue was finally mitigated by making changes to our car design to incorporate the requirements of the Model Block. However, they were added in certain ways which allowed us to easily remove them for the consideration of weight.

We extruded our car body 7mm backward into a solid cuboid. This cuboid had a clear differentiation with the main body, allowing us to make a clean cut at the exact point of contact. Additionally, we added 2 mm at the bottom of the car toward the edges of the model. This allowed for simple sanding and sawing while elevating the CO2 canister position to the required height.

Accomplishing Machining Goals

Through our Machining Plans and use of CAM and CNC, we were fairly confident that we achieved our Machining Goals.

Ensure the car is 50 grams --> Use painting to increase mass to the limit

Ensure apt wall thickness and strong joints --> Use of roughing and finishing plans

Keep tolerances as low as possible --> Sand off the main body till the maximum

Other Manufacturing & Assembly



Manufacturing Process

Examine Manufacturing Body:

The first part of the manufacturing was to examine the received part. This examination was done based on the machining goals. To properly achieve this 4 main bodies were manufactured for our final submission, out of which the best 3 were chosen for submission and finishing.



Fig 9.1: Rejected Car Body with machining Issues

Sanding and Finishing:

Each car received a specific sanding and finishing regimen to ensure a perfect body with minimum machine lines and minimum skin friction. The cars were first sanded by 100-grit sandpaper and then increasing grits to achieve a perfect finish. After sanding, our paint outsourcers, House of Polish, felt that the best way to create a smooth glossy finish would be to use a PVA primer. The porous car soaked up the primer and then coats of paint and clear lacquer were applied to ensure the perfect finish.



Fig 9.2: Prototype finishing process with PPE Equipment

Final Regulation Check:

After the final sanding and finishing process, we conducted scrutineering by ourselves to ensure that our car would abide by the most critical clearance zones and regulations. A set of scrutineering tools were printed using a 3D Printer and accurate vernier calipers were used. Places where our car was not abiding regulations was manually sanded and resealed and painted, ensuring no dimensional changes this time. This way, regulation breaks during manufacturing were minimized.



Fig 9.3: Set of custom printed scrutineering tools

Assembly:

After final regulation check, a custom-made 3D printed assembly jig was used to ensure alignment. This jig contained the negative impression of multiple key components like our nose cone. The joints were first aligned with the jig, removed and then glue was added. They were pressed together and the jig was added back on to ensure the joint was perfectly aligned. Additionally, a mass was added to the particularly weaker joints such as the rear wing, to ensure proper adhesion with the surfaces.

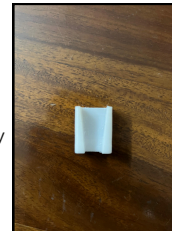


Fig 9.4: Sample of nosecone alignment jig

Joints

Nose Cone Attachment

The attachment of our nose cone was one of the most crucial component joints. The front wing is a pivotal part of our car's aerodynamic efficiency and was printed in one piece along the nosecone to ensure stability. The nosecone was attached using a 3mm hole made in either component and a metal axle was threaded through to ensure strength.

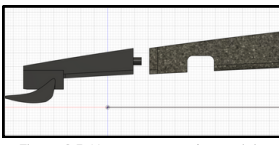


Figure 9.5: Nose cone attachment joint

Rear Wing Attachment

The rear wing was attached using a simple, non-dimensional altering instant bonding adhesive. We could go with this approach as the rear wing joint had a large surface area which wrapped around the CO2 Cartridge chamber. This approach created a strong joint, however needed special alignment tools and precautions to ensure that the wing was in line with the rest of the car body.

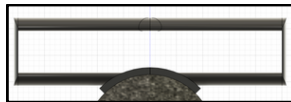


Figure 9.6: Rear wing attachment

Halo Attachment

The halo is the cornerstone of the deceleration system. As a result, the halo undergoes most of the forces for deceleration. To ensure that the halo is secured into its slot, the slot was made slightly smaller (considering machine tolerances) to allow friction to hold the halo in place. Additionally, a strong and lightweight epoxy resin was used to solidify halo placement. The subsequent joint could hold a mass of up to 1 kg without failure.

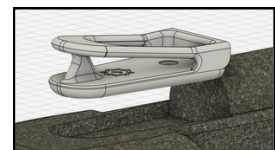


Figure 9.7: Halo attachment

Wheel Support System Attachment

The wheel support system was the same in both the front of the car as well as the rear of the car. Specific slots were machined in the main body of the car which the support system would slide into perfectly, being held in place by friction. Once the alignment was finalized, a little bit of glue was used between the body and the system to ensure its position. Epoxy resin was filled in the hole for the axle and the stationary axle was pushed into it and secured. Additionally, in the case of breakages, a small blade could be used to remove the layer of glue between the main body and system, ensuring replaceability in case of breakages.

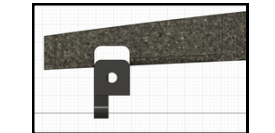


Figure 9.8: Wheel system slot and attachment

Outsourcing

A crucial part of our car design was outsourcing the manufacturing process to professionals. However, this process was quite difficult as there were many cost considerations as well as quality checks. In the end of our project, we decided to rely on outsourcing for 2 main components, choosing to accomplish the remaining aspects inhouse.

Workplace Safety

Risk	Probability	Severity	Causes	Mitigation	Risk Factor
Skin and eye irritation	0.6	0.7	Machine dust, paint fumes	Sanding was conducted in well ventilated areas	0.42
Cuts and flesh wounds	0.2	0.7	Use of hacksaw, drills, undisposed sharp objects	These tasks were always conducted under supervision	0.14
Slipping Hazards	0.2	0.2	Tripping over tools, materials, lubricant	The workplace was always kept organized	0.04
Hearing damage	0.1	0.1	Loud machinery, drills, power tools	Earplugs were utilized around machinery	0.01

Nose Cone Attachment

To ensure the perfect tolerances and finish for our external components, we decided to outsource them to a company called Designifying. Designifying provided us with PA 12 parts made using SLS technology for the best tolerances. However, we could also print our own parts using our own 3D printer. A make v.s. buy analysis was conducted where each criterion has a weight based on importance and is scored out of 5.

Criteria	Weight	Make Score	Make Weighted	Buy Score	Buy Weighted
Quality	5	2	10	5	25
Failure Risk	5	2	10	5	25
Cost per Part	4	5	20	3	12
Time Savings	3	5	15	3	9

Our analysis showed that buy outperformed make by 16 points, making it the obvious choice.

Rapid Prototyping:

We required a way to manufacture the components used for rapid prototyping, joint ideation, and track testing. Our make v.s. buy analysis showed make to be the obvious choice, outperforming buy by roughly 20 points.



Figure 9.9: Nose cone prototypes

Our last aspect for outsourcing was our cars paint job and finish. Although we tried to do this ourselves, we were unable to achieve the surface finish compared to our outsourcers, House of Polish. Although the cost is generally much higher for outsourcing, the make v.s. buy analysis indicated that outsourcing was the better option by 7 points.



Figure 9.10: House of Polish Finish on our Nationals car

Design Evaluation



Development Cycle

Design Conceptualization

The first step in conceptualizing our design was to understand the function of each component in the car as outlined by the technical regulations. Unlike our approach during the national finals, where we primarily drew inspiration from other successful teams at the world level, this time, we adopted a holistic perspective. We took inspiration from a diverse range of sources, including fighter jets, rockets, and real-world Formula One cars. This broader perspective allowed us to create a more innovative and tailored design.

Removal Of Catamaran Effect

Throughout this process we ended up making numerous changes to our design concepts. One of them being the Catamaran Concept.

The Catamaran Concept was one of the major innovations utilized in our national finals car. We took inspiration from Catamaran Boats and used under channels to direct fluid away from our car.

However we found that this approach increased the area of exit air, negatively impacting the car's aerodynamic efficiency. Hence, the consideration of this effect was removed from all of our conceptualizations.

Venturi Effect

The Venturi effect was attempted in this car body by designing it with a narrow midsection that gradually widens toward the rear. From the top view, you can see how the body tapers in the center, which was intended to create an area of reduced pressure as air moves through the narrowed section and then expands outwards. This design aimed to accelerate airflow through the constricted area, decreasing pressure in line with the Venturi principle. The goal was to generate a smoother and faster airflow under the car, thereby enhancing downforce and stability by controlling pressure distribution along the body.

However, the results of this approach were not reflective of its intent and we noticed 0-marginal changes in velocity in each section of the main body during simulations.

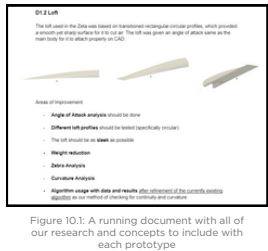


Figure 10.2: Our inspiration for the Catamaran Concept

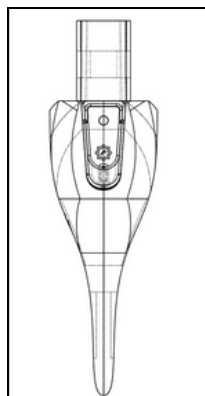


Figure 10.3: Application of the venturi effect

Initial Designing and CAD Modelling

The initial design phase began with hand-drawn sketches to better visualize and conceptually outline the car we intended to create. Multiple perspectives were sketched to help us understand the extrusions and sketching order required in CAD modeling. This structured approach ensured we could work efficiently in Fusion 360, minimizing the steps in the timeline to make it easier to access and edit each component as needed. We kept the primary regulations in mind while designing; however, some minor adjustments were made later to adhere to additional standards, ensuring the car met all specifications.

Stationary Axles

One major decision made during our modelling process was about stationary axles. After seeing the effect of rotating axles on the moment of inertia and the increased risks associated with it, it was decided to go ahead with stationary axles.

Removal of Loft

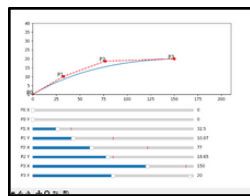


Figure 10.5: Our loft model to create the most optimal shape

Throughout our national finals tenure, we were abiding by the old regulations. In these sets of regulations, a major component was always the loft. We created an entire regression-based model to create the most optimal loft profiles for a diffuser shape. However, we needed to make a decision this year about whether to keep the loft or not. We decided that the loft would not be worth the addition of mass for making the structure and we would be better served by cutting mass everywhere else in the car.

Aerodynamic Simulation and Iterations

With the initial model ready, we imported it as a STEP file into SolidWorks to conduct Computational Fluid Dynamics (CFD) analysis. This testing allowed us to assess drag values, downforce, and airflow patterns around each component of the car. The SolidWorks Flow Simulation add-in provided insights into areas where drag was excessive, enabling us to make informed modifications, such as smoothing body contours and adjusting wing angles. Feedback from mentors was instrumental in guiding these adjustments, helping us to fine-tune the car's aerodynamics based on both qualitative and quantitative data from the simulations.

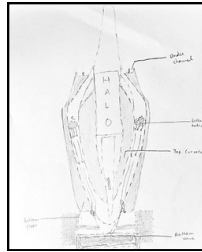


Figure 10.4: Hand drawn model of the car

Deeming Channeled Sidepods Redundant

A critical decision after simulations was the requirement of channeled sidepods. Throughout National Finals, we had sidepods which channeled the air away from our car. However through the simulations we realized that this was quite redundant. The fluid mass flow is so miniature at this scale that it didn't really make a large difference.

Hence, to optimize our mass reduction we chose to go with only hollowed sidepods rather than channeled. This increased the simplicity of the design and also aided us in the process of managing all the separate channels of air on the car.

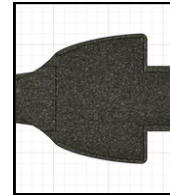


Figure 10.6: The underbody profile with only hollowed out sidepods

Use of tapered-conical nose cone

A tapered nose cone was integrated into the main body as it reduced the frontal surface area, reduced drag and weight as well. It was given a profile similar to that of a bullet to ensure it's aerodynamically stable and efficient.



Figure 10.7: Model of our tapered-conical nose cone

The tapered surface helps generate downforce as well which is needed for the rolling motion of the tires with the ground. It also provides a smooth transition of the air from the ground towards the upper main body. Tapering also reduces weight and gives the nose cone a sleek and streamlined profile

Weight Reduction and Optimization

Through this phase, we recognized the critical role that weight plays at the small scale of F1 in Schools cars. Many aerodynamic features have marginal or negligible impacts at this scale, making weight minimization a priority.

Mass vs Aerodynamics

With our experience in National Finals, we decided that mass played a much larger role in performance. Even though our drag value had decreased significantly from the earlier prototypes, since the mass was 4 grams higher the car performance stayed relatively the same, if not worse. Through this experience, we learnt the importance of mass in our car. Moving forward we incorporated mass-cutting philosophies throughout our car design.

Final Car Summary

Drag: 0.3 N

Track Testing: 0.831 s



Figure 10.8: Final Car Model